

Assessment of major ions and heavy metals in groundwater: a case study from Guangzhou and Zhuhai of the Pearl River Delta, China

Yintao LU (✉)¹, Changyuan TANG², Jianyao CHEN³, Hong YAO¹

¹ School of Civil Engineering, Beijing Jiaotong University, Beijing 100044, China

² Faculty of Horticulture, Chiba University, Chiba 271-8510, Japan

³ School of Geography and planning, Sun Yat-sen University, Guangzhou 510275, China

© Higher Education Press and Springer-Verlag Berlin Heidelberg 2015

Abstract Anthropogenic activities in the Pearl River Delta (PRD) have caused a deterioration of groundwater quality over the past twenty years as a result of rapid urbanization and industrial development. In this study, the hydrochemical characteristics, quality, and sources of heavy metals in the groundwater of the PRD were investigated. Twenty-five groundwater samples were collected and analyzed for pH, electrical conductivity (EC), total dissolved solids (TDS), $\delta^{18}\text{O}$, $\delta^2\text{H}$, major ions, and heavy metals. The groundwater was slightly acidic and presented TDS values that ranged from 35.5 to 8,779.3 $\text{mg}\cdot\text{L}^{-1}$. The concentrations of the major ions followed the order $\text{Cl}^- > \text{HCO}_3^- > \text{Na}^+ > \text{SO}_4^{2-} > \text{NO}_3^- > \text{NH}_4^+ > \text{Ca}^{2+} > \text{K}^+ > \text{Mg}^{2+} > \text{Fe}^{2+/3+} > \text{Al}^{3+}$. Ca-Mg- HCO_3 and Na-K- HCO_3 were the predominant types of facies, and the chemical composition of the groundwater was primarily controlled by chemical weathering of the basement rocks, by mixing of freshwater and seawater and by anthropogenic activities. The heavy metal pollution index (HPI) indicated that 64% of the samples were in the low category, 16% were in the medium category and 20% were in the high category, providing further evidence that this groundwater is unsuitable for drinking. Lead, arsenic, and manganese were mainly sourced from landfill leachate; cadmium from landfill leachate and agricultural wastes; mercury from the discharge of leachate associated with mining activities and agricultural wastes; and chromium primarily from industrial wastes. According to the irrigation water quality indicators, the groundwater in the PRD can be used for irrigation in most farmland without strong negative impacts. However, approximately

9 million people in the Guangdong Province are at risk due to the consumption of untreated water. Therefore, we suggest that treating the groundwater to achieve safer levels is necessary.

Keywords Pearl River Delta, groundwater quality, hydrochemical type, sodium salts accumulation, heavy metal pollution

1 Introduction

Globally, rapid urbanization in various watersheds has caused severe environmental pollution, particularly in water quality (Erturk et al., 2010; Fan et al., 2012; Haloi and Sarma, 2012). Water quality has therefore been a focus of governments and scientists. The Pearl River Delta (PRD), which has rich water resources, is located in South China and is one of the most highly industrialized regions in China. The water supply of this region consists of both surface water and groundwater due to abundant rainfall and a well-developed river network. The PRD has experienced a rapid population increase and economic growth, particularly over the last twenty years. Although there are abundant water resources in the PRD, anthropogenic activities in this region have generated large amounts of pollutants that have been directly and indirectly discharged into the rivers and groundwater (Ouyang et al., 2006; Ni et al., 2008). All groundwater samples with salinities of $> 10 \text{ g}\cdot\text{L}^{-1}$ are located within 56 km of the sea in the southern part of the PRD (Wang and Jiao, 2012). However, approximately 25% of rural people in the Guangdong Province still drink groundwater directly without any treatment, which is a direct risk for human

health.

The contamination of groundwater by heavy metals pose a serious and continuous health risk to humans. Heavy metals present at trace concentrations play a major role in the metabolism and healthy growth of plants and animals. However, increased concentrations of heavy metals may have several toxicological effects on humans (Purushotham et al., 2013). In recent years, a considerable amount of concern has been expressed globally regarding the contamination of groundwater by heavy metals due to rapid industrialization and urbanization. Various natural and anthropogenic sources, such as atmospheric deposition, geological weathering, agricultural activities, residential and industrial products, and corrosion products from the soil, can lead to the presence of heavy metals in groundwater. Because of the rapid urbanization of the PRD, most of the aforementioned sources are potential sources for heavy metals, thus making the evaluation of heavy metals dissolved in the groundwater in this region extremely important.

The sources and quality of the groundwater in the PRD have attracted increasing attention in recent years. In some studies, stable isotopes used as tracers for the surface water recharge of groundwater, and hydrogeochemical diagrams such as Piper third-line diagrams, have been used (Wang and Jiao, 2012; Wang et al., 2013b; Yuan et al., 2013). The quality of groundwater can be influenced by the dry fallout of atmospheric particulate matter, by the chemical weathering of rocks and soils (Wang and Jiao, 2012; Wang et al., 2013a), by the mixing of freshwater and seawater (Wang et al., 2013b) and by anthropogenic sources (Huang et al., 2011; Liu et al., 2011; Wang et al., 2012). Studies have been conducted on trace metal contamination in the PRD, but these studies have focused on the surface sediment and river water of the Pearl River Estuary or on only As in the groundwater (Huang et al., 2011; Liu et al., 2011; Wang et al., 2012). For example, the accumulation of heavy metals and nutrients in the sediments and river water of the PRD region was studied by Cheung et al. (2003). Huang et al. (2011) reported that As in some groundwater samples from certain sewage irrigation areas in the PRD area exceeded the upper limit for drinking water established by the World Health Organization. However, few studies have investigated the concentrations, distributions, and sources of trace elements in the groundwater of the PRD. In particular, previous studies have examined the occurrence and concentration of As in groundwater of the PRD, but this region may be susceptible to contamination by trace elements other than As, such as Cr and Cd. These trace elements have not yet been explored, despite their important health implications. Therefore, the objective of this work was to determine the hydrochemical characteristics and heavy metal pollution of the groundwater and to assess the quality of the groundwater for agricultural and domestic uses.

2 Materials and methods

2.1 Site descriptions

Geologically, the Pearl River drainage basin was formed by the uplift of the Tibetan Plateau during the Tertiary and Quaternary periods (Aitchison et al., 2007). The delta began to develop in the Late Pleistocene epoch and is situated on the Cathaysian tectonic block. The basement rocks include shale, sandstone, limestone, dolomite, granite, and gneiss, ranging in age from Cambrian to Tertiary (GHT, 1981). Because of the humid-warm climatic conditions of the PRD, the soil profile is relatively deficient in soluble salts, alkali metals, and alkali-earth metals but is rich in Fe and Al oxides (Lan et al., 2003). The delta has been influenced by several transgressive events since the early Pleistocene (Wang et al., 2013a). There are many terraces in the PRD, and the highest is the fifth-stage terrace. It is largely covered with Quaternary sediments, which primarily consist of clay, silty clay, and fine sand, and has a thickness of 25 m in the north, increasing to 60 m near the coast (Zong et al., 2009). The PRD has an elevation ranging from 6 to 9 m above sea level near the north to 1–2 m near the coast (GHT, 1981).

The study area consists of two regions of the PRD: Guangzhou and Zhuhai (Fig. 1). Guangzhou formed earlier than the Zhuhai area through the actions of the Beijiang River and Dongjiang River, and there are many flats and hills. The sediment layer is primarily composed of sand and clay, and hardpan can be found in some areas. Permian limestone lies beneath the sediment layer. There is an abundance of groundwater resources that are used by people in this area. The Zhuhai area is an alluvial plain formed by the Pearl River and now supports a coastal city. This area features the fastest industrial and agricultural growth.

2.2 Water sampling and chemical analysis

A total of 25 shallow groundwater samples were collected in March 2006 from wells after pumping for approximately half an hour and were stored in one-liter polyethylene bottles; 20 (samples A–T) samples are from Guangzhou, and the remaining five (Samples U–Y) samples are from Zhuhai (Fig. 1). Prior to sampling, the polyethylene bottles were thoroughly washed three times with the groundwater, which was filtered through a hand-held filter system using a 0.45 mm cellulose filter paper. Parameters such as pH, temperature, electrical conductivity (EC) and total dissolved solids (TDS) were determined in the field. The pH was determined using a Hach portable pH/ISE meter. The EC, TDS, and temperature were determined using a Hach conductivity meter. The Likeng Landfill is located close to samples T and N (Fig. 1)

The samples were refrigerated at 4°C before being

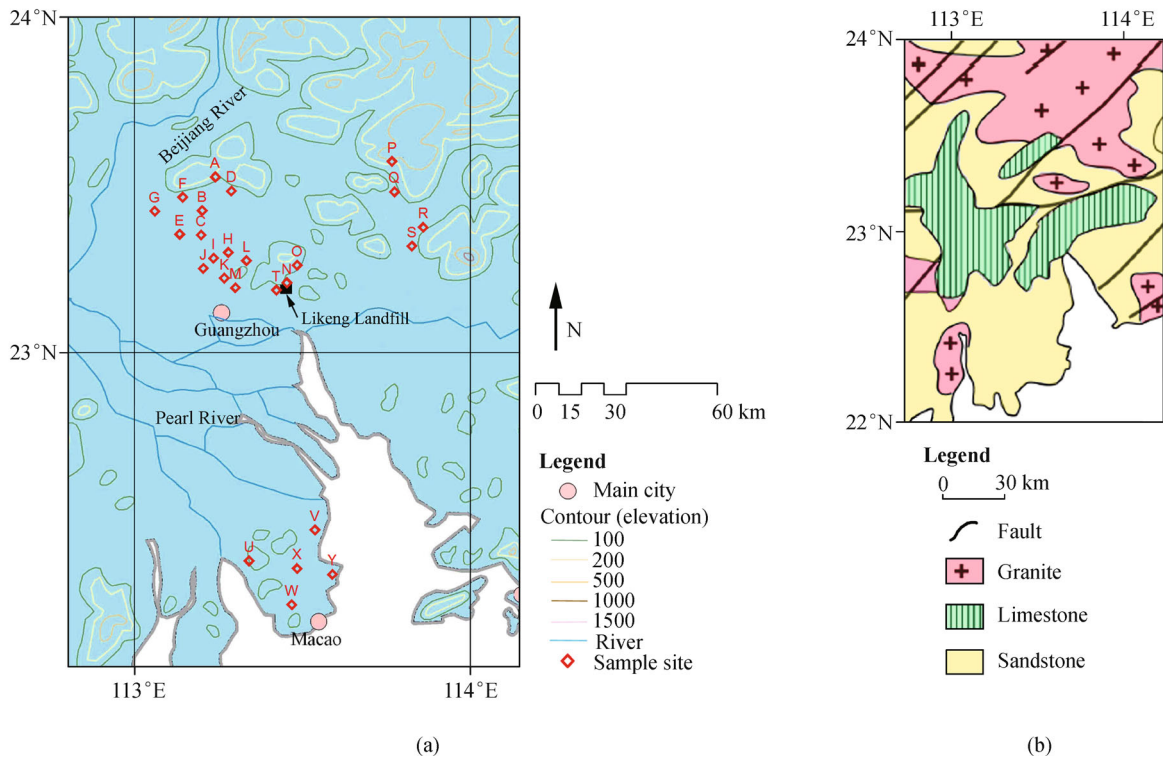


Fig. 1 Study area, sample sites and geological map. (a) Sample sites; (b) geological map of the study area.

transported to Chiba University, Japan, for chemical analysis. Standard laboratory methods were used to determine the other physical and chemical characteristics of the groundwater. The concentrations of K^+ , Na^+ , Ca^{2+} , Mg^{2+} , NH_4^+ , Cl^- , SO_4^{2-} , and NO_3^- were determined using ion chromatography (Shimadzu CTO-10A), and the concentration of HCO_3^- was determined via titration. Stable isotope (^{18}O and 2H) values were determined using a mass spectrometer (Finnigan MAT Delta S). For the oxygen isotopic analysis, approximately 10 mL of each water sample were equilibrated with CO_2 by shaking for 6 hours at $25^\circ C$ (Kelln et al., 2001; Li et al., 2008). For the hydrogen isotopic analysis, metallic zinc was used to produce hydrogen gas via the zinc-reduction method. Pb and Cd were determined by graphite furnace atomic absorption spectrometry (AAS). Hg and As were determined using atomic fluorescence spectroscopy (AFS). Mn, Fe, and Al were determined using flame atomic absorption spectroscopy (FAAS), and Cr^{6+} was determined using 1,5-diphenylcarbohydrazide spectrophotometry.

2.3 Statistical analysis

Principal component analysis (PCA), which is commonly used in environmental impact studies, reduces the complexity of large-scale geochemical data sets making it easier to identify common underlying processes (Ayuba et al., 2013). PCA was performed on the geochemical data

using the software package SPSS Statistics 19. In the PCA, the principal components were calculated based on the correlation matrix, and a Varimax with Kaiser Normalization was used. The contour maps of heavy metals were developed using Surfer 8 software with Kriging interpolation methods.

2.4 Assessment of groundwater quality

To understand the overall quality of water with respect to the selected parameters, the Heavy metal Pollution Index (HPI) was used. The HPI is an overall quality index that reflects the composite influence of a number of individual heavy metal characteristics. The HPI is calculated using the following formula (Mohan et al., 1996; Sajil Kumar et al., 2012):

$$HPI = \left[\sum_{i=1}^n Q_i \times W_i \right] / \sum_{i=1}^n W_i, \quad (1)$$

where Q_i is the sub index of the i^{th} parameter, W_i is the unit weight of the i^{th} parameter, and n is the number of parameters (types of heavy metals). The sub index (Q_i) of the parameter is calculated as follows:

$$Q_i = \sum_{i=1}^n [|(M_i - I_i)|] / [|(S_i - I_i)|] \times 100, \quad (2)$$

where M_i is the concentration value of the heavy metal of the i^{th} parameter, I_i is the ideal value of the i^{th} parameter, and S_i is the standard value of the i^{th} parameter.

The hydrochemical parameters of groundwater used to classify and determine suitability for irrigation are EC and sodium percentage (Na%). The sodium percentage (Na%) in the water samples was calculated using the following equation:

$$\text{Na\%} = \frac{\text{Na}}{\text{Ca} + \text{Mg} + \text{Na} + \text{K}} \times 100. \quad (3)$$

Sodium-rich salts accumulate in the soil through capillary transport and evaporation. The sodium or alkali hazard associated with using the water for irrigation was determined using the absolute and relative concentrations of cations and was expressed in terms of the sodium adsorption ratio (SAR; Bhardwaj and Singh, 2011). The SAR was estimated using the following equation:

$$\text{SAR} = \frac{\text{Na}}{\sqrt{\frac{(\text{Ca} + \text{Mg})}{2}}}. \quad (4)$$

The ion concentrations in Eqs. (3) and (4) are molar concentrations.

3 Results and discussion

3.1 Statistical analysis of water chemistry

The results of the analysis of the hydrochemical parameters are presented in Table 1. The pH of the surface and groundwater samples ranged from 5.28 to 7.85, with a mean value of 6.47, indicating slightly acidic conditions. Approximately 48% of the pH values were within the prescribed limits of 6.5 to 8.5 for potable water, which were set as health guidelines by the World Health Organization (WHO, 1993), but 52% of the water is not fit to drink. The TDS varied from 35.5 $\text{mg}\cdot\text{L}^{-1}$ to 8,779.3 $\text{mg}\cdot\text{L}^{-1}$, with a mean of 651.3 $\text{mg}\cdot\text{L}^{-1}$. The TDS values in four groundwater samples were above the stipulated guideline limit of 500 $\text{mg}\cdot\text{L}^{-1}$ for drinking water. Groundwater that contains $> 1,000 \text{ mg}\cdot\text{L}^{-1}$ of TDS (only one sample) may have laxative or constipation effects. The mean concentrations of anions follow the order $\text{Cl}^- > \text{HCO}_3^- > \text{SO}_4^{2-} > \text{NO}_3^-$, the mean concentrations of cations follow the order $\text{Na}^+ > \text{NH}_4^+ > \text{Ca}^{2+} > \text{K}^+ > \text{Mg}^{2+} > \text{Fe}^{2+/3+} > \text{Al}^{3+}$, and the mean concentrations of trace elements follow the order $\text{Mn}^{2+} > \text{Cr}^{6+} > \text{Hg}^{1+/2+} > \text{Pb}^{2+} > \text{As}^+ > \text{Cd}^{2+}$.

Table 1 Drinking water quality guidelines (WHO) and statistical analysis of chemical component for the groundwater in the PRD ($n = 25$)

Water quality index	Mean	Median	Min.	Max.	WHO guideline value (1993, 2011)	No. of sample above the stipulated value
pH	6.47	6.36	5.28	7.85	6.5–8.5	
TDS/($\text{mg}\cdot\text{L}^{-1}$)	651.25	359.86	35.46	8,779.31	500	4
Pb ²⁺ /($\mu\text{g}\cdot\text{L}^{-1}$)	1.41	0.10	–	14.15	10	1
Cd ²⁺ /($\mu\text{g}\cdot\text{L}^{-1}$)	0.06	–	–	0.55	3	0
Hg ^{1+/2+} /($\mu\text{g}\cdot\text{L}^{-1}$)	1.84	–	–	11.55	1	8
As ⁺ /($\mu\text{g}\cdot\text{L}^{-1}$)	0.69	0.30	0.05	4.30	10	0
Mn ²⁺ /($\mu\text{g}\cdot\text{L}^{-1}$)	160.00	120.00	–	740.00	100	13
Cr ⁶⁺ /($\mu\text{g}\cdot\text{L}^{-1}$)	11.56	9.00	4.00	39.00	50	0
Fe ^{2+/3+} /($\text{mg}\cdot\text{L}^{-1}$)	1.40	0.15	–	15.38	0.3	9
Al ³⁺ /($\text{mg}\cdot\text{L}^{-1}$)	0.91	0.46	0.13	5.10	0.2	25
Cl ⁻ /($\text{mg}\cdot\text{L}^{-1}$)	239.81	28.19	0.16	4,934.25	250	2
HCO ₃ ⁻ /($\text{mg}\cdot\text{L}^{-1}$)	95.27	92.75	–	245.29	–	
SO ₄ ²⁻ /($\text{mg}\cdot\text{L}^{-1}$)	56.99	26.17	1.41	629.83	250	1
NO ₃ ⁻ /($\text{mg}\cdot\text{L}^{-1}$)	52.49	17.22	–	272.11	50	7
Na ⁺ /($\text{mg}\cdot\text{L}^{-1}$)	98.03	22.20	5.26	1,711.84	200	1
K ⁺ /($\text{mg}\cdot\text{L}^{-1}$)	38.04	9.51	1.60	634.86	–	
Mg ²⁺ /($\text{mg}\cdot\text{L}^{-1}$)	16.99	3.91	0.23	276.57	–	
Ca ²⁺ /($\text{mg}\cdot\text{L}^{-1}$)	45.71	40.73	1.42	124.58	–	
NH ₄ ⁺ /($\text{mg}\cdot\text{L}^{-1}$)	45.67	1.95	0.19	1,006.52	1.5	15

Table 2 Correlation coefficient matrix of water quality parameters ($n = 25$)

	Pb	Cd	Hg	As	Mn	Cr	Fe	Al	Cl	HCO ₃	SO ₄	NO ₃	Na	K	Mg	Ca	NH ₄
Pb	1.000																
Cd	0.501	1.000															
Hg	0.050	-0.154	1.000														
As	0.569	0.342	-0.234	1.000													
Mn	-0.050	-0.138	-0.248	0.193	1.000												
Cr	0.606	0.371	-0.021	0.724	-0.076	1.000											
Fe	0.407	0.391	-0.120	0.718	0.074	0.701	1.000										
Al	0.540	0.362	-0.072	0.766	0.083	0.719	0.969	1.000									
Cl	-0.099	-0.108	-0.058	-0.122	0.237	-0.058	-0.056	-0.041	1.000								
HCO ₃	0.027	-0.119	-0.339	-0.005	-0.038	0.036	0.133	0.100	0.230	1.000							
SO ₄	-0.109	-0.053	-0.098	-0.181	0.194	-0.099	-0.060	-0.065	0.959	0.359	1.000						
NO ₃	-0.118	0.042	-0.009	-0.259	0.118	-0.251	-0.193	-0.122	0.632	-0.094	0.564	1.000					
Na	-0.098	-0.102	-0.065	-0.124	0.237	-0.063	-0.054	-0.038	0.999	0.228	0.958	0.656	1.000				
K	-0.105	-0.102	-0.078	-0.147	0.203	-0.071	-0.068	-0.060	0.994	0.285	0.967	0.625	0.994	1.000			
Mg	-0.107	-0.119	-0.090	-0.126	0.272	-0.079	-0.063	-0.045	0.995	0.224	0.956	0.667	0.996	0.988	1.000		
Ca	-0.106	-0.169	-0.324	-0.195	0.217	-0.218	-0.041	0.011	0.501	0.530	0.562	0.609	0.515	0.501	0.559	1.000	
NH ₄	-0.092	-0.097	-0.049	-0.117	0.228	-0.045	-0.046	-0.036	0.998	0.244	0.964	0.595	0.996	0.993	0.990	0.472	1.000

The correlation matrix for major ions and heavy metals is presented in Table 2, and the correlation between parameters was considered to be significant at values equal to or greater than 0.5 (Ayuba et al., 2013). Cl⁻ exhibited a very strong correlation (0.959) with SO₄²⁻, indicating that the two anions were likely derived from the same source. Na⁺-Cl⁻, K⁺-Cl⁻, Mg²⁺-Cl⁻, NH₄⁺-Cl⁻, Ca²⁺-Cl⁻, Ca²⁺-HCO₃⁻, Na⁺-SO₄²⁻, K⁺-SO₄²⁻, Ca²⁺-SO₄²⁻, NH₄⁺-SO₄²⁻, NH₄⁺-NO₃⁻, Na⁺-K⁺, Na⁺-Mg²⁺, Na⁺-Ca²⁺, Na⁺-NH₄⁺, K⁺-Ca²⁺, and Mg²⁺-NH₄⁺ were also significantly correlated pairs, indicating that all major ionic components, except HCO₃⁻, influence each other. Wang and Jiao (2012) reported that $\delta^{13}\text{C}$ values increase with increasing HCO₃⁻ concentrations, which confirms that HCO₃⁻ is significantly influenced by methanogenesis.

In this study, 17 parameters in 25 groundwater samples were used for the PCA, and four principal components (PCs) were extracted. These PCs explained 81% of the total sample variance. Significant PCs were selected based on the Kaiser criterion with eigenvalues greater than one and a total explained percentage of variation equal to or greater than 70% (Ayuba et al., 2013). Table 3 presents the factor loadings, the latent root, the eigenvalue and the percentage of variation of each PC. The selection of parameters for each PC was based on its latent root; the first PC had a latent root of 7.0, the second had a latent root of 3.9, the third had a latent root of 1.6, and the fourth had a latent root of 1.1. Nine parameters were considered to be highly varied for PC1, six for PC2, two for PC3 and one for PC4.

Table 3 Factor loadings of each variance

Parameter ($n = 25$)	PC1	PC2	PC3	PC4
Mg	0.978	0.151	0.098	-0.048
Na	0.973	0.160	0.132	-0.018
K	0.971	0.146	0.109	0.037
Cl	0.969	0.160	0.137	-0.016
NH ₄	0.961	0.169	0.143	0.000
SO ₄	0.956	0.139	0.034	0.101
NO ₃	0.706	-0.057	0.192	-0.074
Ca	0.645	0.030	-0.503	0.134
Al	-0.176	0.905	-0.025	0.030
Fe	-0.187	0.874	-0.078	0.020
As	-0.275	0.836	-0.059	-0.236
Cr	-0.232	0.827	0.155	0.102
Pb	-0.219	0.671	0.200	0.171
Cd	-0.186	0.505	0.218	-0.151
Hg	-0.114	-0.205	0.731	0.147
HCO ₃	0.299	0.177	-0.681	0.526
Mn	0.257	0.135	-0.283	-0.828
Latent roots	6.983	3.910	1.569	1.141
Percentage variation	41.08	23.00	9.23	6.71

The first PC (PC1) explained 41.1% of the total sample variance and featured a loading of Na⁺, Mg²⁺, K⁺, Cl⁻, Ca²⁺, NH₄⁺, SO₄²⁻, and NO₃⁻. Cl⁻ was one of the most

abundant major ions in the groundwater samples and it was considered to be from a marine source; the differences in Cl^- in different samples were likely due to variations in the seawater contribution (Wang and Jiao, 2012). The concentrations of Na^+ , K^+ , Mg^{2+} and Ca^{2+} in the groundwater indicated weathering of plagioclase-bearing rocks or another hydrogeochemical process, such as freshwater/seawater mixing (Wang and Jiao, 2012). SO_4^{2-} is associated with the abundant authigenic pyrite identified in Quaternary sediments from the PRD (Lan, 1991; Wang and Jiao, 2012). Without significant nitrification, the concentrations of NH_4^+ in groundwater should primarily be influenced by sorption, which is primarily controlled by cation-exchange processes in porous media (Buss et al., 2004; Jiao et al., 2010). PC1 could therefore be said to reflect the influence of natural sources.

The second PC (PC2), which described 23% of the total variance, featured a high loading of As^+ , Cr^{6+} , $\text{Fe}^{2+/3+}$, Al^{3+} , Cd^{2+} and Pb^{2+} . $\text{Fe}^{2+/3+}$ and Al^{3+} are hypothesized to be released by the weathering of ferromagnesian micas and granites in the basement rocks (Fig. 1(b)). The Cd pollution in the groundwater was likely derived from multiple sources, including agricultural runoff from heavily polluted soils resulting from the widespread use of agrochemicals and pesticides that contain Cd in the region (Luo et al., 2014), atmospheric deposition (Wong et al., 2003), and industrial wastewater (Wong et al., 2007). The burning of coal by power generation plants, automobile exhaust, and some industrial activities (such as Pb-Zn ore deposit mining or smelting) in the region may be the major source of Pb, which entered the groundwater via atmospheric inputs (Liu et al., 2011). In addition to the

arsenic-rich pyrite that has been generally considered to be the dominant source of dissolved arsenic in groundwater (Schreiber et al., 2000), the concentrations of As^+ and Cr^{6+} also reflect an anthropogenic source from mining activities and agricultural industrial wastes in the Guangdong Province. Thus, the association of these elements in PC2 revealed that the groundwater was contaminated with trace elements.

PC3 accounted for 9.2% of the total variance of the data set and featured a high loading of HCO_3^- and $\text{Hg}^{1+/2+}$. HCO_3^- may be due to the action of CO_3^{2-} on the basic material of soils and granitic rocks. $\text{Hg}^{1+/2+}$ is from volcanic leaching (Beal et al., 2014) and anthropogenic activities (Shi et al., 2010). This PC reflects carbonate changes and mercury pollution in the groundwater.

PC4 accounted for 6.7% of the total variance of the data set and featured a high loading of Mn^{2+} . Mn^{2+} is hypothesized to be released by the weathering of bedrock material (mica, biotite and amphibole hornblende).

3.2 Identification of groundwater provenance and chemistry

Water isotopic data are useful for elucidating the atmospheric moisture sources and the meteorological and geographical factors responsible for rain formation (Zhang et al., 2013, 2014). A local meteoric water line (LMWL) for the study area provided the basis for the interpretation in this study. The LMWL (Fig. 2(a)) is represented by the isotope composition of precipitation (data from the IAEA), and the equation is $\delta^2\text{H} = 8.32\delta^{18}\text{O} - 11.98$ (correlation coefficient: $R^2 = 0.99$). The isotope values ranged between -50‰ and -35‰ for $\delta^2\text{H}$ and

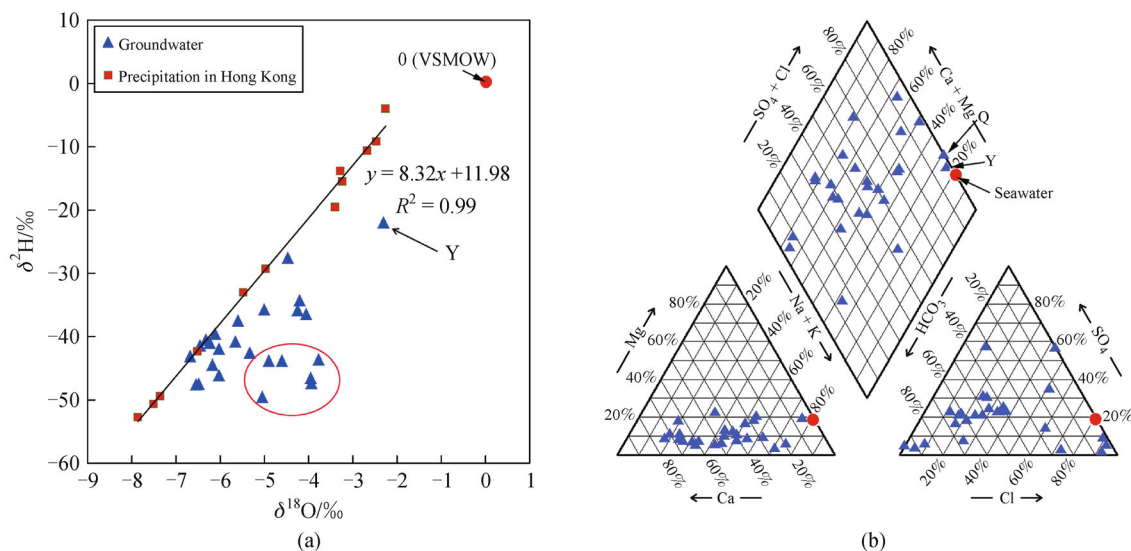


Fig. 2 (a) Plot of $\delta^{18}\text{O}$ and $\delta^2\text{H}$ values of the groundwater. The solid line is the local meteoric water line. (b) Piper diagram of groundwater in the PRD.

between -6.5% and -3.5% for $\delta^{18}\text{O}$. As shown in Fig. 2(a), the isotopic composition of most groundwater (except sample Y) in the study area falls below the LMWL in a narrow range, confirming that the groundwater should be characterized by the precipitation source. However, the enrichments of $\delta^2\text{H}$ and $\delta^{18}\text{O}$ (falling in the red circle in Fig. 2(a)) are hypothesized to be the result of water-rock exchange (Lu et al., 2008). The $\delta^{18}\text{O}$ values of modern surface seawater in the South China Sea are between -0.2% and 0.5% (Sue, 2001), very close to the 0% of VSMOW. The most enriched $\delta^{18}\text{O}$ and $\delta^2\text{H}$ samples are from sample Y, located close to the sea, and its $\delta^{18}\text{O}$ and $\delta^2\text{H}$ values indicate significant marine influence.

A plot developed by Piper (1944) was used to infer the hydrochemical types of groundwater. The Piper plot (Fig. 2 (b)) revealed four hydrochemical types (Ca-Mg- HCO_3 , Ca-Mg-Cl- SO_4 , Na-K- HCO_3 , and Na-K-Cl- SO_4), and the predominant types were Ca-Mg- HCO_3 and Ca-Mg-Cl- SO_4 .

The Ca-Mg- HCO_3 type is described as alkaline earth water. This type constitutes approximately 48% of the total samples in the area. Because Ca^{2+} , Mg^{2+} , and HCO_3^- commonly result from the weathering of granite (Fig. 1(b); Wang and Jiao, 2012), this type most likely reflects the dissolution of dolomite and granitic minerals in the bedrock. The Ca-Mg-Cl- SO_4 type falls within the alkaline earth water and constitutes approximately 40% of the samples, indicating that the groundwater of these sites may have formed via similar hydrochemical processes. In the study area, these groundwater samples (samples C, I, J, K, and H) were collected from a plain area in the middle of the groundwater flow system. In this area, the groundwater reactions are dominated by ion-exchange and evaporation (Zhao et al., 2007). The Na-K- HCO_3 and Na-K-Cl- SO_4 types represent approximately 12% of the total samples. The Na-K- HCO_3 type is an alkaline water type and is usually referred to as “exchange water” because of geochemical evolution through the exchange processes (Ayuba et al., 2013). The occurrence of Cl^- and SO_4^{2-} reveals that the groundwater was influenced by seawater (Wang et al., 2013b) and that Na^+ and K^+ were released from the weathering of silicate minerals from the bedrock (Stallard and Edmond, 1983). Sample Y is located on the coast (Fig. 1) and belongs to the Na-Cl type. In general, NaCl-type water indicates a strong seawater influence in coastal areas. This result is similar to Fig. 2(a).

3.3 Distribution of trace elements

The test analysis performed using SPSS cannot reveal spatial variations or variance structure. However, these can be achieved by generating a contour map, which illustrates the relationship between the sample variance and sample distance and distinguishes between random and spatial variance components. Figure 3 shows that the zones with

higher concentrations of lead ($> 14 \mu\text{g}\cdot\text{L}^{-1}$), arsenic ($> 4.5 \mu\text{g}\cdot\text{L}^{-1}$), and manganese ($> 40 \text{mg}\cdot\text{L}^{-1}$) are located in the same zone. The chemical profile suggested that landfill leachate was the primary pollution source of lead, arsenic, and manganese. In the study area, the background soil manganese concentration was high (Liang et al., 2009), which also contributed to these high levels. The zones with higher concentrations of cadmium ($> 0.55 \mu\text{g}\cdot\text{L}^{-1}$) were located close to the landfill and agricultural region 1 (Fig. 3(g)), likely indicating that the cadmium is sourced from landfill leachate and agricultural sources (Wong et al. 2002; Luo et al., 2014). The zones with higher concentrations of mercury ($> 10 \mu\text{g}\cdot\text{L}^{-1}$) were located close to the mining area and agricultural region 2 (Fig. 3(g)), likely indicating that the mercury is from mining activities and agricultural sources (Lin et al., 2007). The zones with higher concentrations of chromium were located in town areas, and there is a factory located near the highest chromium concentration, suggesting that the chromium is primarily from industrial wastes, such as leather and electroplating wastewater production (Cai et al., 2009).

The HPI represents the composite influence of metals on the overall quality of water (Sheykhi and Moore, 2012). In this index, weights (W_i) between 0 and 1 are assigned for each metal. The rating is based on the relative importance of individual quality considerations and is defined as inversely proportional to the permissible standard for each heavy metal (Mohan et al., 1996). The parameters S_i , I_i , and W_i are presented in Table 4. Although Hg and As are not heavy metals, they have certain heavy metal characteristics, such as high toxicity and refractory degradation. Therefore, Hg and As are treated as heavy metals. The HPI for the study area was determined by incorporating the average values of the recorded trace elements. The mean HPI was 45.14, and the individual values are shown in Fig. 4. HPI values can be classified into three categories: low (< 19), medium (19–38), and high (> 38) (Sajil Kumar et al., 2012); a high HPI value indicates that the groundwater has been polluted with trace elements. The majority of the samples (64%) fall into the low category, and the remainder of the samples belong to the medium and high categories. The highest values were recorded for samples G, P, S, W, and X, suggesting that urbanization and industrialization have affected the groundwater quality. The high HPI values were located next to agricultural pollution sources, mining pollution sources, and the coast (Fig. 1 and Fig. 3(g)).

3.4 Groundwater quality for drinking and irrigation purposes

Table 1 presents a comparison of the results from the physiochemical analysis of the groundwater of the study area with standard guideline values recommended by the

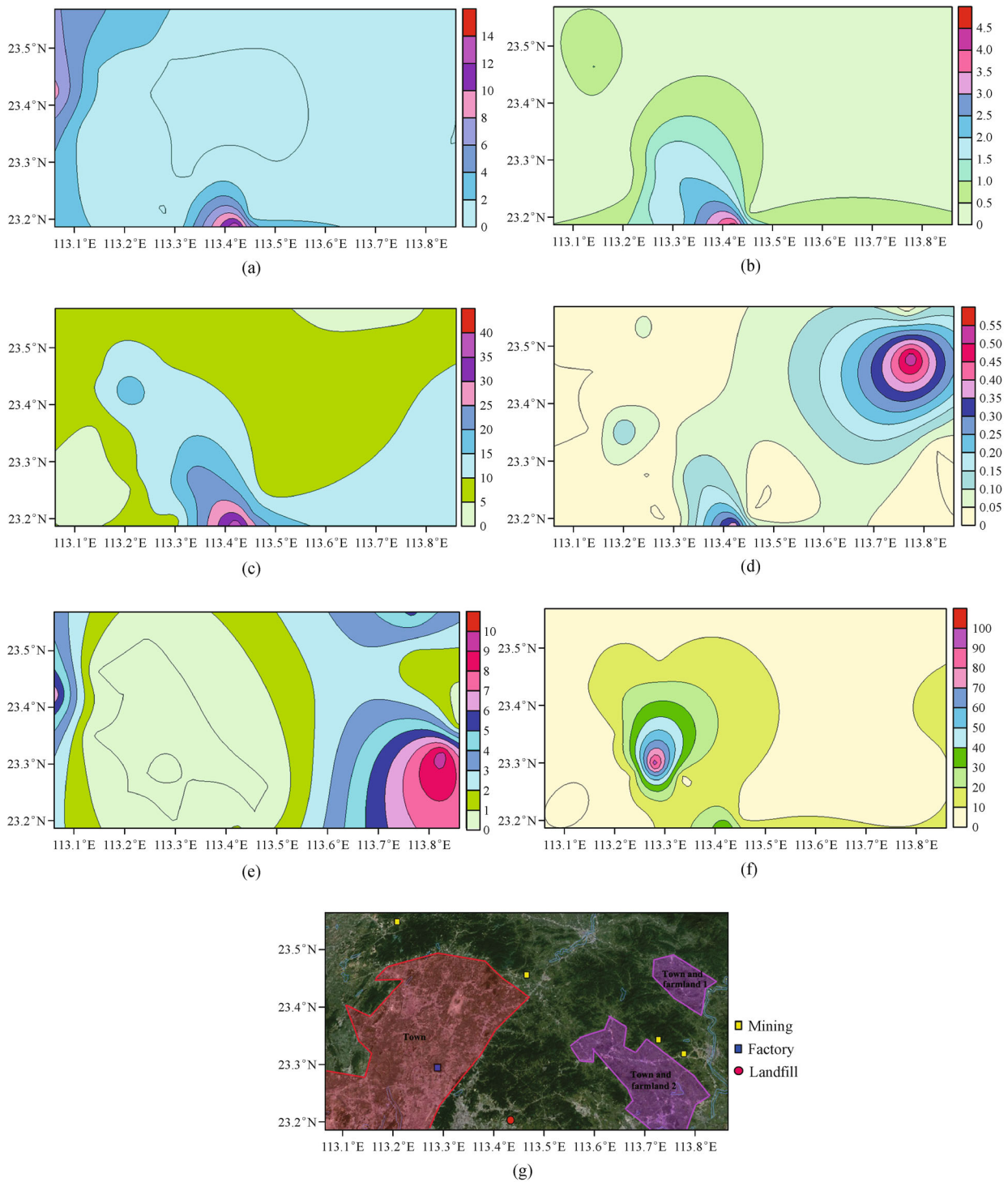
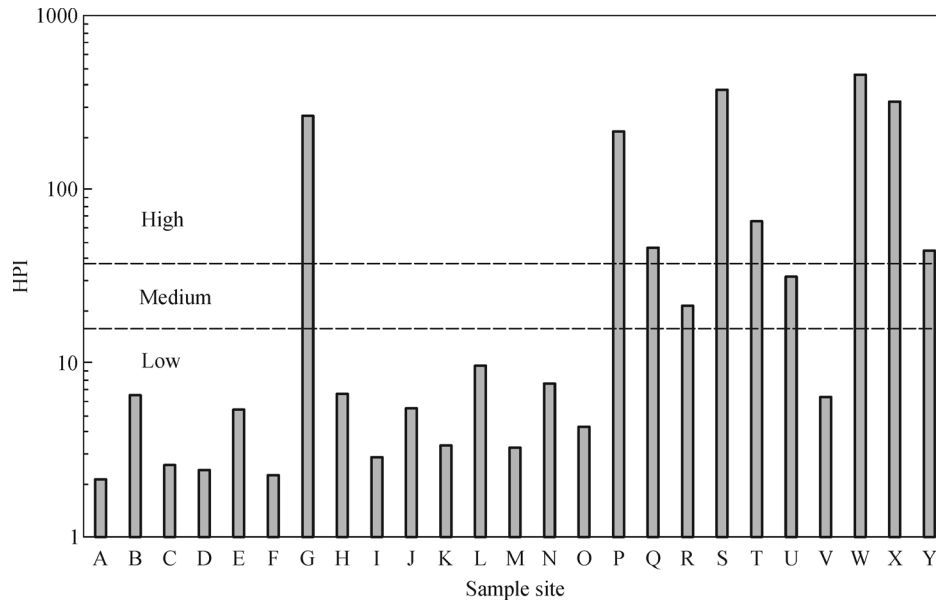


Fig. 3 Spatial variation maps showing trace element concentration in the study area. (a) Pb($\mu\text{g}\cdot\text{L}^{-1}$); (b) As($\mu\text{g}\cdot\text{L}^{-1}$); (c) Mn($\text{mg}\cdot\text{L}^{-1}$); (d) Cd($\mu\text{g}\cdot\text{L}^{-1}$); (e) Hg($\mu\text{g}\cdot\text{L}^{-1}$); (f) Cr($\mu\text{g}\cdot\text{L}^{-1}$); (g) distribution of point and surface source.

Table 4 The main parameters of heavy metal pollution index (HPI)

Heavy metal	Standard permissible value/($\mu\text{g}\cdot\text{L}^{-1}$) (S_i)	Highest desirable value/($\mu\text{g}\cdot\text{L}^{-1}$) (I_i)	Unit weight (W_i)
Pb	50	10	0.02
Cd	10	–	0.1
Hg*	10	–	0.1
As*	10	–	0.1
Mn	500	100	0.002
Cr	50	10	0.02

*Although Hg and As are not heavy metals, they have some heavy metal characteristics, such as high toxicity and refractory degradation. Therefore, Hg and As are treated as heavy metals.

**Fig. 4** HPI values for the individual groundwater samples.

WHO (1993, 2011) for drinking water purposes. The results indicated that 16% of the samples presented TDS values above the guideline value of $500 \text{ mg}\cdot\text{L}^{-1}$, and 4%, 32%, and 52% of the samples were contaminated with the trace elements Pb^{2+} , $\text{Hg}^{1+/2+}$, and Mn^{2+} , respectively. All (100%) of the groundwater samples had concentrations of the trace metal Al^{3+} above the stipulated guideline values and 36% had higher than guideline values for $\text{Fe}^{2+/3+}$. In addition, 32% and 60% of the groundwater samples contained concentrations of NO_3^- and NH_4^+ , respectively, above the stipulated guideline values, suggesting that the groundwater was influenced by urbanization processes. The majority of the groundwater samples had concentrations of Cl^- , SO_4^{2-} and Na^+ that were below the guideline values for drinking water.

Salinization is the major cause of loss of production and is one of the most prolific adverse environmental impacts associated with irrigation. Saline conditions severely restrict the choice of crops, adversely affect crop germination and yields, and can pollute the soils (Bhardwaj and

Singh, 2011). The Na% in the area ranged from 14.27% to 69.06%. Na% values greater than 35% in groundwater are unsuitable for irrigation (Vasanthavigar et al., 2010). Approximately 40% of the groundwater samples presented Na% values lower than 35% and were suitable for irrigation purposes. The plot of Na% versus EC (Wilcox, 1955) shows that the groundwater samples were of excellent to doubtful quality (Fig. 5(a)). Only three samples of groundwater fell into the category of good to permissible, suggesting that these water types may be used for irrigation purposes.

There is a significant relationship between the SAR values of irrigation water and the extent to which sodium is absorbed by the soils. If water used for irrigation is high in sodium and low in calcium, the cation-exchange complex may become saturated with sodium, which can destroy the soil structure due to the dispersion of clay particles. The SAR values ranged from 0.37 to 19.45 (sample Y). SAR values greater than 2.0 indicate that groundwater is unsuitable for irrigation purposes (Vasanthavigar et al.,

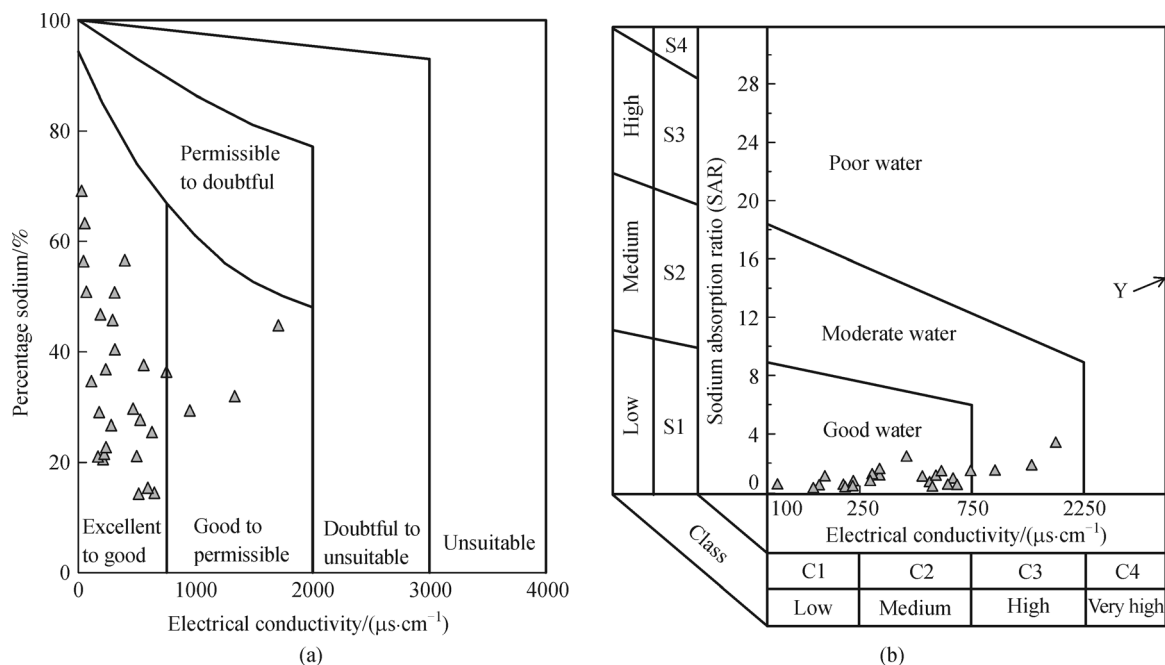


Fig. 5 (a) Plot of Na% versus electrical conductance (Wilcox diagram); (b) U.S. salinity classification of groundwater for irrigation in the study area.

2010). Only groundwater samples I, Q, and Y, with SAR values of 3.5, 2.6, and 19.5, respectively, were unsuitable for irrigation. According to the US salinity diagram classification of irrigation water (USSL, 1954), groundwater falling in the fields C1-S1, C2-S1 and C3-S1 (Fig. 5(b)) represent a low to high salinity hazard and a low sodium (alkalinity) hazard. This groundwater can be used for irrigation with most soil and crops without a strong negative impact.

4 Conclusions

The chemical composition of the groundwater in the PRD was strongly influenced by the effective weathering of plagioclase and granitic rocks underlying the study area, along with anthropogenic activities such as domestic waste, automobile emissions, agricultural runoff, and mining in the urban environment. The groundwater was generally contaminated with trace elements and ions that have health concerns. The HPI analysis indicated that 60% of the groundwater samples were in the low category, 8% were in the medium category and 32% were in the high category, indicating that the groundwater in the study area is unsuitable for drinking or for domestic purposes. Lead, arsenic, and manganese were primarily from landfill leachate; cadmium was from landfill leachate and agricultural sources; mercury was from mining activities and agricultural sources; and chromium was likely from industrial wastes. Among the groundwater samples, 32%, 52%, and 16% fall within the low, medium, and high

salinity hazard categories, respectively, though the Wilcox classification indicated that the groundwater can be used for irrigation for most soils and crops without a strong negative impact.

Acknowledgements This study is supported in part by grants from the National Natural Science Foundation of China (Grant No. 41103007), the Fundamental Research Funds for the Beijing Jiaotong University (No. C13JB00070) and Beijing Natural Science Foundation (No. 8142031). The authors express that great thanks to the anonymous reviews for their time and efforts.

References

- Aitchison J C, Ali J R, Davis A M (2007). When and where did India and Asia collide? *J Geophys Res, B, Solid Earth*, 112(5): 1–2
- Ayuba R, Omonona O V, Onwuka O S (2013). Assessment of groundwater quality of Lokoja Basement Area, North-Central Nigeria. *J Geol Soc India*, 82(4): 413–420
- Beal S A, Kelly M A, Stroup J S, Jackson B P, Lowell T V, Tapia P M. (2014). Natural and anthropogenic variations in atmospheric mercury deposition during the Holocene near Quelccaya Ice Cap, Peru. *Global Biogeochem Cycles*, 28(4): 437–450
- Bhardwaj V, Singh D S (2011). Surface and groundwater quality characterization of Deoria District, Ganga Plain, India. *Environmental Earth Sciences*, 63(2): 383–395
- Buss S R, Herbert A W, Morgan P, Thornton S F, Smith J W N (2004). A review of ammonium attenuation in soil and groundwater. *Quarterly Journal of Engineering Geology and Hydrogeology*, 37(4): 347–359
- Cai L M, Huang L C, Zhou Y Z, Ma J, Du H Y, Dou L, Zhang C B

- (2009). The spatial structure and distribution of Cr contents in agricultural soils in a typical area of the Pearl River Delta, China. *Journal of Agro-Environment Science*, 28(1): 60–65 (in Chinese)
- Cheung K C, Poon B H T, Lan C Y, Wong M H (2003). Assessment of metal and nutrient concentrations in river water and sediment collected from the cities in the Pearl River Delta, South China. *Chemosphere*, 52(9): 1431–1440
- Erturk A, Gurel M, Ekdal A, Tavsan C, Ugurluoglu A, Seker D Z, Tanik A, Ozturk I (2010). Water quality assessment and meta model development in Melen watershed–Turkey. *J Environ Manage*, 91(7): 1526–1545
- Fan X Y, Cui B S, Zhang Z M (2012). Spatial variations of river water quality in Pearl River Delta, China. *Front Earth Sci*, 6(3): 291–296
- GHT (1981). Regional Hydrogeological Survey Report. Guangzhou: Guangdong Hydrogeological Team (in Chinese)
- Haloï N, Sarma H P (2012). Heavy metal contaminations in the groundwater of Brahmaputra flood plain: an assessment of water quality in Barpeta District, Assam (India). *Environ Monit Assess*, 184(10): 6229–6237
- Huang G X, Sun J C, Zhang Y, Jing J H, Zhang Y X, Liu J T (2011). Distribution of arsenic in sewage irrigation area of Pearl River Delta, China. *Journal of Earth Science*, 22(3): 396–410
- Jiao J J, Wang Y, Cherry J A, Wang X S, Zhi B F, Du H Y, Wen D G (2010). Abnormally high ammonium of natural origin in a coastal aquifer–aquitard system in the Pearl River Delta, China. *Environ Sci Technol*, 44(19): 7470–7475
- Kelln C J, Wassenaar L I, Hendry M J (2001). Stable isotopes ($\delta^{18}\text{O}$, $\delta^2\text{H}$) of pore waters in clay-rich aquitards: a comparison and evaluation of measurement techniques. *Ground Water Monit Remediat*, 21(2): 108–116
- Lan H X, Hu R L, Yue Z Q, Lee C F, Wang S J (2003). Engineering and geological characteristics of granite weathering profiles in South China. *J Asian Earth Sci*, 21(4): 353–364
- Lan X (1991). Sedimentary characteristics and strata division of core 22 of the Zhujiang River Delta. *Oceanol Limnol Sin*, 22(2): 148–154
- Li F D, Pan G Y, Tang C Y, Zhang Q Y, Yu J J (2008). Recharge source and hydrogeochemical evolution of shallow groundwater in a complex alluvial fan system, southwest of North China Plain. *Environmental Geology*, 55(5): 1109–1122
- Liang G L, Sun J C, Huang G X, Jing J H, Liu J T, Chen X, Zhang Y X, Du H Y (2009). Origin and distribution characteristics of manganese in groundwater of the Pearl River Delta. *Geology in China*, 36(4): 899–906 (in Chinese)
- Lin J F, Lai Q H, Fang J W, Ma S M (2007). Appraise of environmental geochemistry in soil Hg polluted areas in the Pearl River Delta. *Ecol Environ*, 16(1): 41–46 (in Chinese)
- Liu B L, Hu K, Jiang Z L, Yang J, Luo X M, Liu A H (2011). Distribution and enrichment of heavy metals in a sediment core from the Pearl River Estuary. *Environmental Earth Sciences*, 62(2): 265–275
- Lu Y T, Tang C Y, Chen J Y, Sakura Y (2008). Impact of septic tank systems on local groundwater quality and water supply in the Pearl River Delta, China: case study. *Hydrol Processes*, 22(3): 443–450
- Luo X L, Guo Q R, Xie Z Y, Yang J J, Chai Z W, Liu X, Wu S F (2014). Study on heavy metal pollution in typical rural soils in Pearl River Delta area. *Ecology and Environmental Sciences*, 23(3): 485–489 (in Chinese)
- Mohan S V, Nithila P, Reddy S J (1996). Estimation of heavy metal in drinking water and development of heavy metal pollution index. *J Environ Sci Health A*, 31(2): 283–289
- Ni H G, Lu F H, Luo X L, Tian H Y, Zeng E Y (2008). Riverine inputs of total organic carbon and suspended particulate matter from the Pearl River Delta to the coastal ocean off South China. *Mar Pollut Bull*, 56(6): 1150–1157
- Ouyang T P, Zhu Z Y, Kuang Y Q (2006). Assessing impact of urbanization on river water quality in the Pearl River Delta Economic Zone, China. *Environ Monit Assess*, 120(1–3): 313–325
- Piper A M (1944). A graphic procedure in the geochemical interpretation of water analyses. *Eos, Transactions American Geophysical Union*, 25(6): 914–928
- Purushotham D, Rashid M, Lone M A, Rao A N, Ahmed S, Nagaiah E, Dar F A (2013). Environmental impact assessment of air and heavy metal concentration in groundwater of Maheshwaram Watershed, Ranga Reddy District, Andhra Pradesh. *J Geol Soc India*, 81(3): 385–396
- Sajil Kumar P J, Davis Delson P, Thomas Babu P (2012). Appraisal of heavy metals in groundwater in Chennai City using a HPI model. *Bull Environ Contam Toxicol*, 89(4): 793–798
- Schreiber M E, Simo J A, Freiberg P G (2000). Stratigraphic and geochemical controls on naturally occurring arsenic in groundwater, eastern Wisconsin, USA. *Hydrogeol J*, 8(2): 161–176
- Sheykhi V, Moore F (2012). Geochemical characterization of Kor River water quality, Fars Province, Southwest Iran. *Water Quality, Exposure and Health*, 4(1): 25–38
- Shi J B, Ip C C M, Zhang G, Jiang G B, Li X D (2010). Mercury profiles in sediments of the Pearl River Estuary and the surrounding coastal area of South China. *Environ Pollut*, 158(5): 1974–1979
- Stallard R F, Edmond J M (1983). Geochemistry of the Amazon river: 2. The influence of the geology and weathering environment on dissolved load. *J Geophys Res*, 88(C14): 9671–9688
- Sue F H (2001). Depth Distributions of $\delta^{18}\text{O}$ and Changes in Mixed Layer Thickness in the South China Sea. Dissertation for Master degree. National Sun Yat-sen University (in Chinese)
- USSL (1954). Diagnosis and improvement of saline and alkali soils. Washington DC: USDA Handbook No. 60
- Vasanthavignar M, Srinivasamoorthy K, Vijayaragavan K, Rajiv Ganthi R, Chidambaram S, Anandhan P, Manivannan R, Vasudevan S (2010). Application of water quality index for groundwater quality assessment: Thirumanimuttar sub-basin, Tamil Nadu, India. *Environ Monit Assess*, 171(1–4): 595–609
- Wang D L, Lin W F, Yang X Q, Zhai W D, Dai M H, Chen C T A (2012). Occurrences of dissolved trace metals (Cu, Cd, and Mn) in the Pearl River Estuary (China), a large river-groundwater-estuary system. *Cont Shelf Res*, 50–51: 54–63
- Wang X S, Jiao J J, Wang Y, Cherry J A, Kuang X X, Liu K, Lee C, Gong Z J (2013a). Accumulation and transport of ammonium in aquitards in the Pearl River Delta (China) in the last 10,000 years: conceptual and numerical models. *Hydrogeol J*, 21(5): 961–976
- Wang Y, Jiao J J (2012). Origin of groundwater salinity and hydrogeochemical processes in the confined Quaternary aquifer of the Pearl River Delta, China. *J Hydrol (Amst)*, 438–439: 112–124
- Wang Y, Jiao J J, Cherry J A, Lee C M (2013b). Contribution of the

- aquitard to the regional groundwater hydrochemistry of the underlying confined aquifer in the Pearl River Delta, China. *Sci Total Environ*, 461–462: 663–671
- WHO (1993). *Guidelines for drinking water quality* (2nd ed). Recommendations, Geneva: World Health Organization, 188
- WHO (2011). *Guidelines for drinking-water quality world health organization* (4th ed). Geneva: World Health Organization, 340
- Wilcox L V (1955). *Classification and use of irrigation waters* (1st ed). Washington DC: United States Department of Agriculture
- Wong C S C, Li X D, Zhang G, Qi S H, Min Y S (2002). Heavy metals in agricultural soils of the Pearl River Delta, South China. *Environ Pollut*, 119(1): 33–44
- Wong C S C, Li X D, Zhang G, Qi S H, Peng X Z (2003). Atmospheric deposition of heavy metals in the Pearl River Delta, China. *Atmos Environ*, 37(6): 767–776
- Wong C S C, Wu S C, Duzgoren-Aydin N S, Aydin A, Wong M H (2007). Trace metal contamination of sediments in an e-waste processing village in China. *Environ Pollut*, 145(2): 434–442
- Yuan J F, Mao X M, Wang Y X (2013). Hydrogeochemical characteristics of low to medium temperature groundwater in the Pearl River Delta region, China. *Procedia Earth and Planetary Science*, 7: 928–931
- Zhang Y, Li F D, Li J, Liu Q, Zhao G S (2013). Quantitative estimation of groundwater recharge ratio along the riparian of the Yellow River. *Water Sci Technol*, 68(11): 2427–2432
- Zhang Y, Li F D, Zhao G S, Li J, Zhu Q Y (2014). An attempt to evaluate the recharge source and extent using hydrogeochemistry and stable isotopes in North Henan Plain, China. *Environ Monit Assess*, 186(8): 5185–5197
- Zhao X F, Chen J Y, Tang C Y, Zeng S Q, Lu Y T (2007). Hydrochemical characteristics and evolution of groundwater in a small catchment of Pearl River Delta. *Ecol Environ*, 16(6): 1620–1626 (in Chinese)
- Zong Y, Yim W W S, Yu F, Huang G (2009). Late Quaternary environmental changes in the Pearl River Mouth region, China. *Quat Int*, 206(1–2): 35–45